Three-Dimensional Modeling of High-Latitude Scintillation Observations

[1] **Alex T. Chartier,** [2] Biagio Forte, [3] Kshitija B. Deshpande,
[1] Gary S. Bust, [2] Cathryn N. Mitchell

Beacons Satellite Symposium, 29 June 2016

[1] Johns Hopkins University Applied Physics Laboratory, 11100 Johns Hopkins Road, Laurel MD 20723

[2] Dept. Electronic and Electrical Engineering, University of Bath, Claverton, Bath, UK

[3] Bradley Department of Electrical and Computer Engineering, Virginia Tech, 1901 Innovation Dr., Blacksburg, VA 24061

JOHNS HOPKINS
APPLIED PHYSICS LABORATORY

Summary

- Scintillations observed in high-rate GPS signals provide a means of studying ionospheric behavior beyond the resolution of EISCAT incoherent scatter radar. At GPS frequencies (L1: 1575 MHz, L2: 1228 MHz), intermediate-scale irregularities (approximately 0.1-10 km) are responsible for diffractive scattering.
- Case study: the ionospheric electron density profile is observed by EISCAT incoherent scatter radar (Tromsø) along the same line-of-sight as a scintillating GPS signal
- EISCAT large-scale (10s of km) densities constrain a 3D irregularity model with a multiple phase screen propagation algorithm.
- The observed signal is modeled and likely characteristics of the underlying ionospheric irregularities are estimated

Observational Approach

- Experiment at Tromsø (66.73 N, 102.18 E): EISCAT UHF antenna aimed at GPS satellite PRN 23, beam tracking every 5 minutes. Ground scintillation monitor takes 50 Hz observations

- Scintillations observed just after 20:00 UT (close to midnight magnetic local time) on 17 October 2013

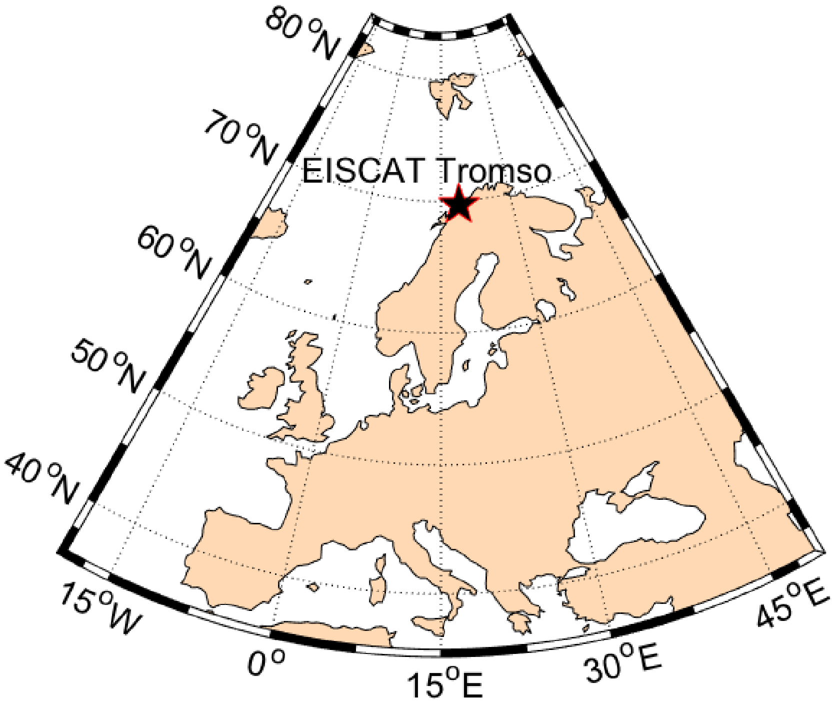

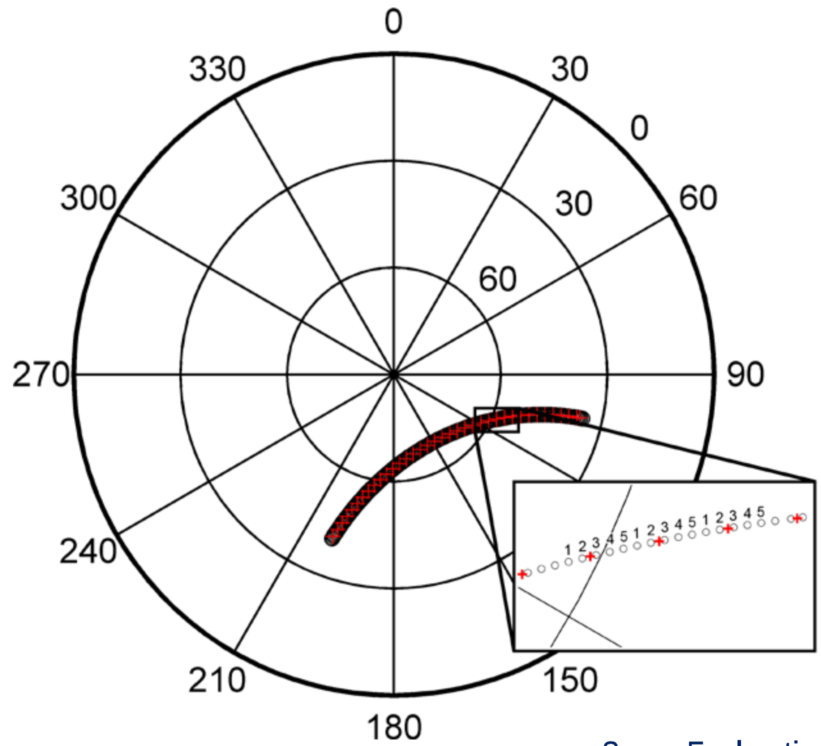

Space Exploration

Observations

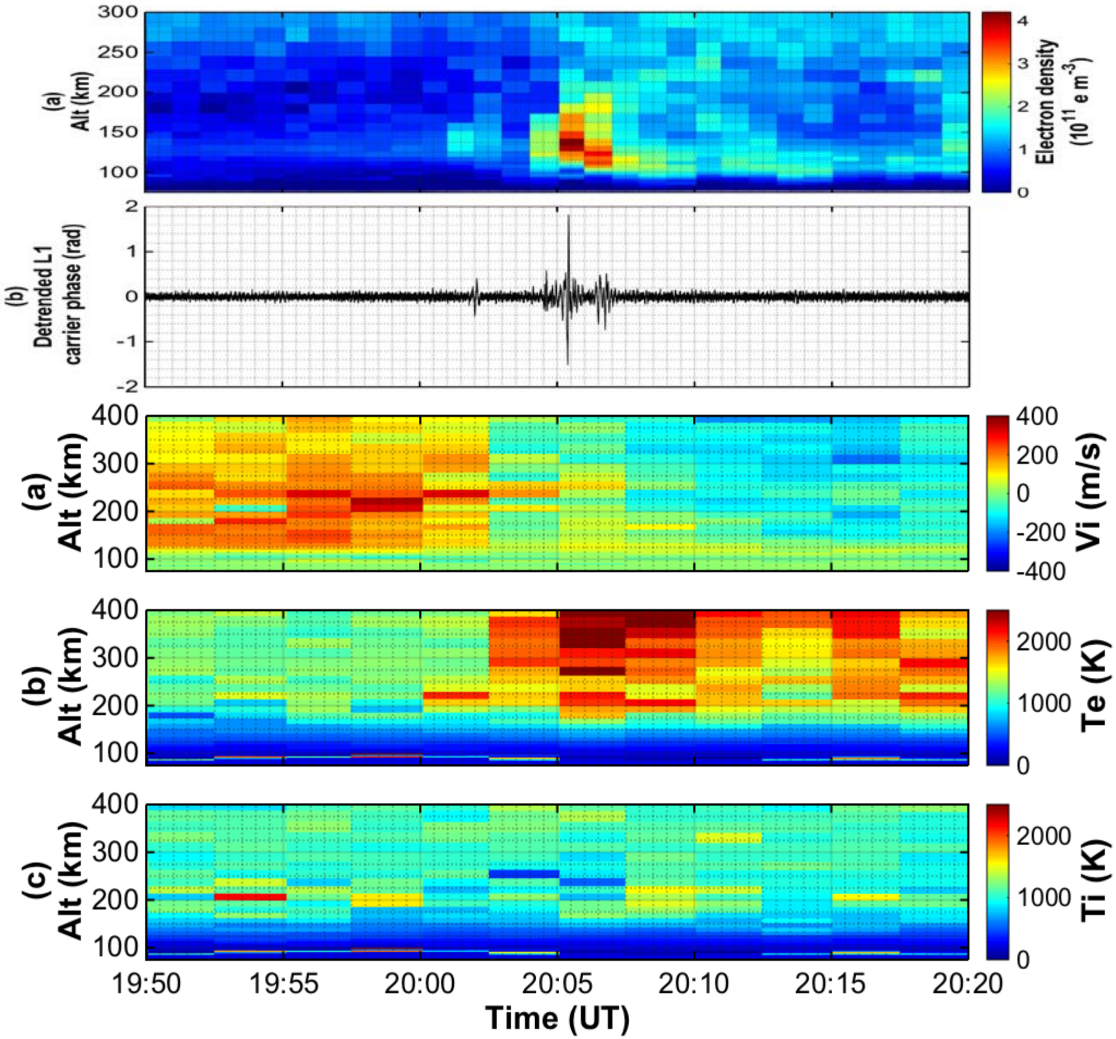

- E-region density enhancement occurs in the auroral zone around midnight MLT (20:05 UT).
- Spike in the detrended 50 Hz GPS carrier phase at the same time.
- Line-of-sight velocities drop to ~100 m/s
- Large (1500 K) electron temperature enhancement characteristic of electron precipitation
- No corresponding ion temperature enhancement

Observations

- Density enhancement associated with a phase spike but no observable intensity

- 50 Hz data detrended using 3rd-order polynomial and 6th-order Butterworth 0.1-Hz high pass filter.

- Power spectral densities calculated using Welch's method with a Hamming window, eight segments and a 50% overlap

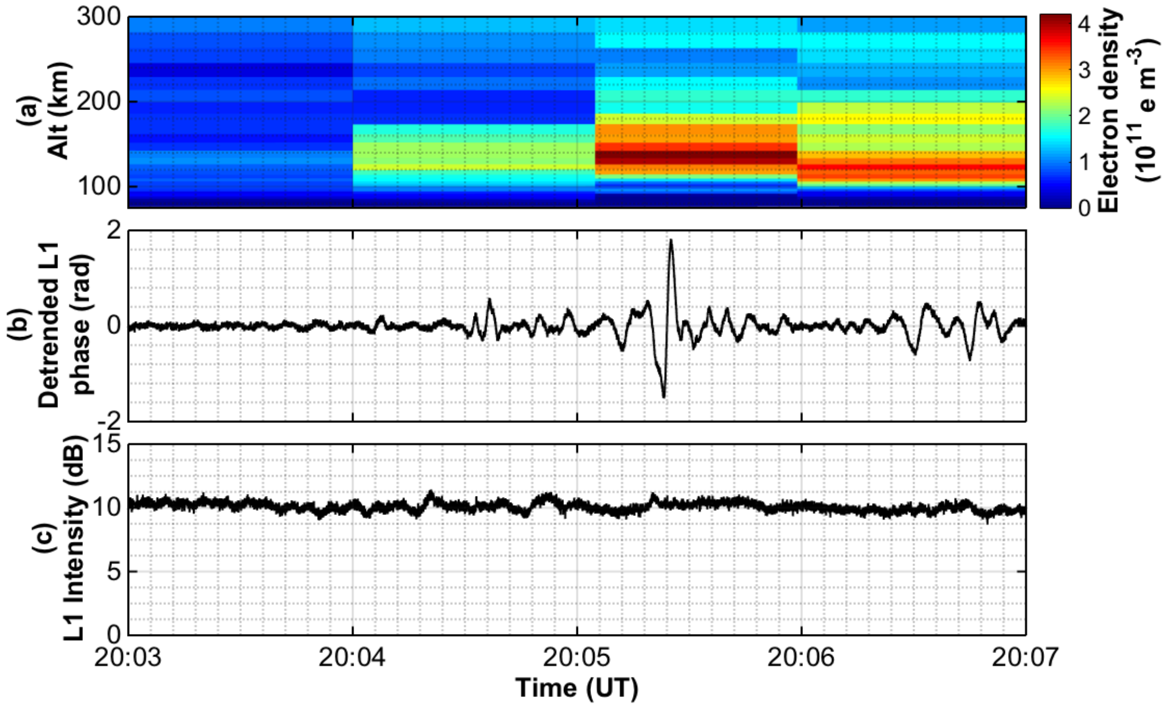

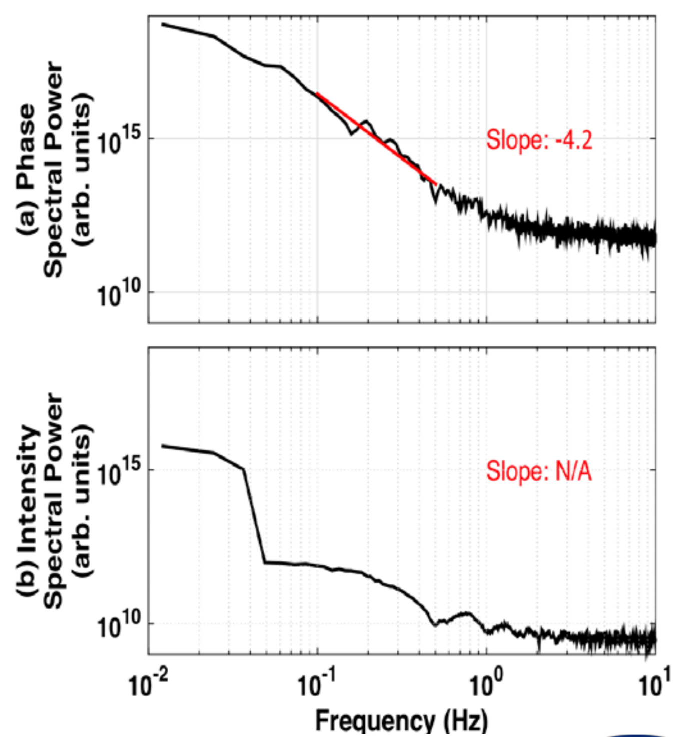

Modeling propagation

- Satellite-beacon Ionospheric scintillation Global Model of the upper Atmosphere (SIGMA) is adapted here
- *Deshpande et al.* [2014] developed the model and performed a comprehensive parametric sensitivity study
- Multiple phase screens constructed to represent signal scattering caused by ionospheric irregularities
- Geometry modification: **Z** along line-of-sight, effective drift velocity is along **Y**

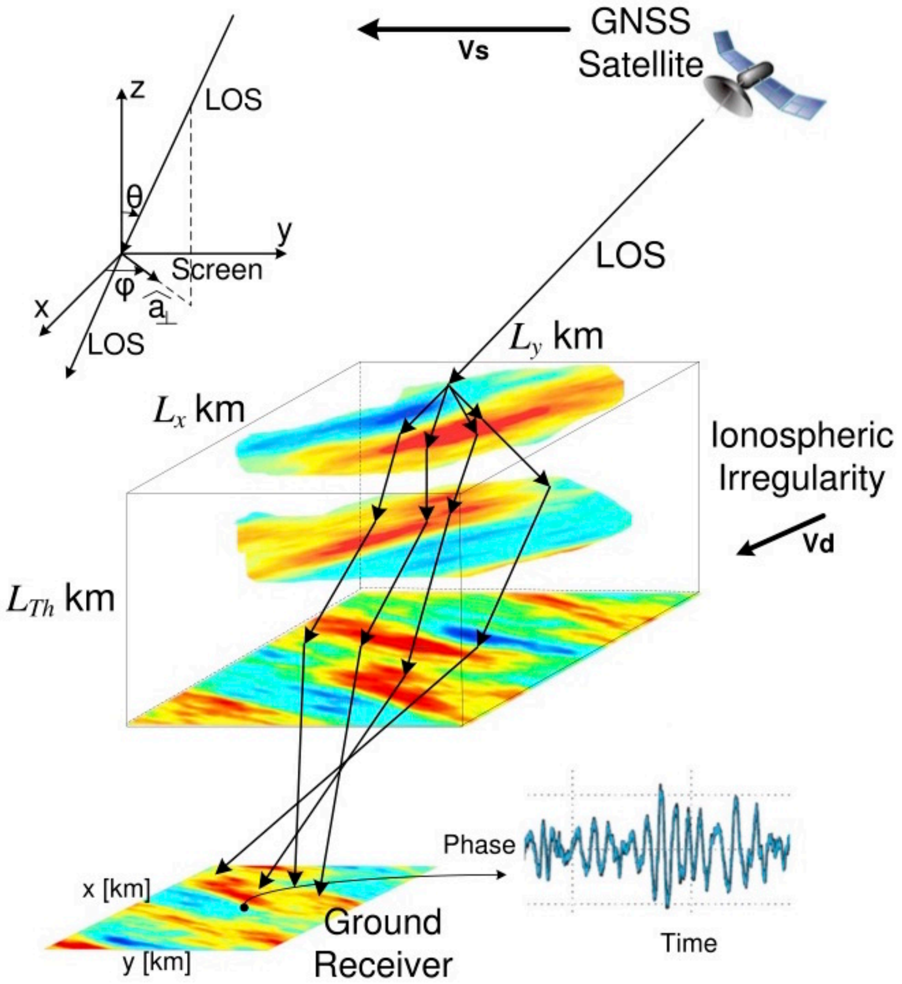

Figure reproduced from *Deshpande et al.* [2014]

Modeling irregularities

Field-aligned irregularity spectrum P(k) is based on the formulation of *Costa and Kelley* [1977]:

$$P(k) = a\,\gamma\,\sin(3\pi/\gamma)\,/\,(4\pi^2 k_0^3)\,\Delta N^2 \cdot \{\,(1 + (k_{x'}^2 + k_{y'}^2 + a^2 k_{z'}^2)\,/\,k_0^2\,)^{-\gamma/2}\,\}^{-1}$$

$k = (k_{x'}, k_{y'}, k_{z'})$: spatial wave number vector, γ: spectral index, *a*: axial ratio, ΔN: root-mean-square density fluctuation, k_0: outer scale wavenumber, z': magnetic field direction.

- Grid defined between 95-175 km altitude (110 – 200 km range)
- Mean electron density N specified to match EISCAT, but fractional fluctuation density $\Delta N/N$ allowed to vary. Effective velocity set to 300 m/s, X/Y extent is 3 km.
- We found *a* > 1 leads to intensity scintillation enhanced above what is observed, so we set a = 1 and therefore $\gamma = 4.2$ (matching observed spectral value)
- Spectral irregularities do not reproduce large (3 radians p-2-p) spike, so kilometer-scale irregularity added at 20:05:25
- 50 random realizations account for ‘chance’ variabiltiy

Space Exploration APL

Model irregularity configuration

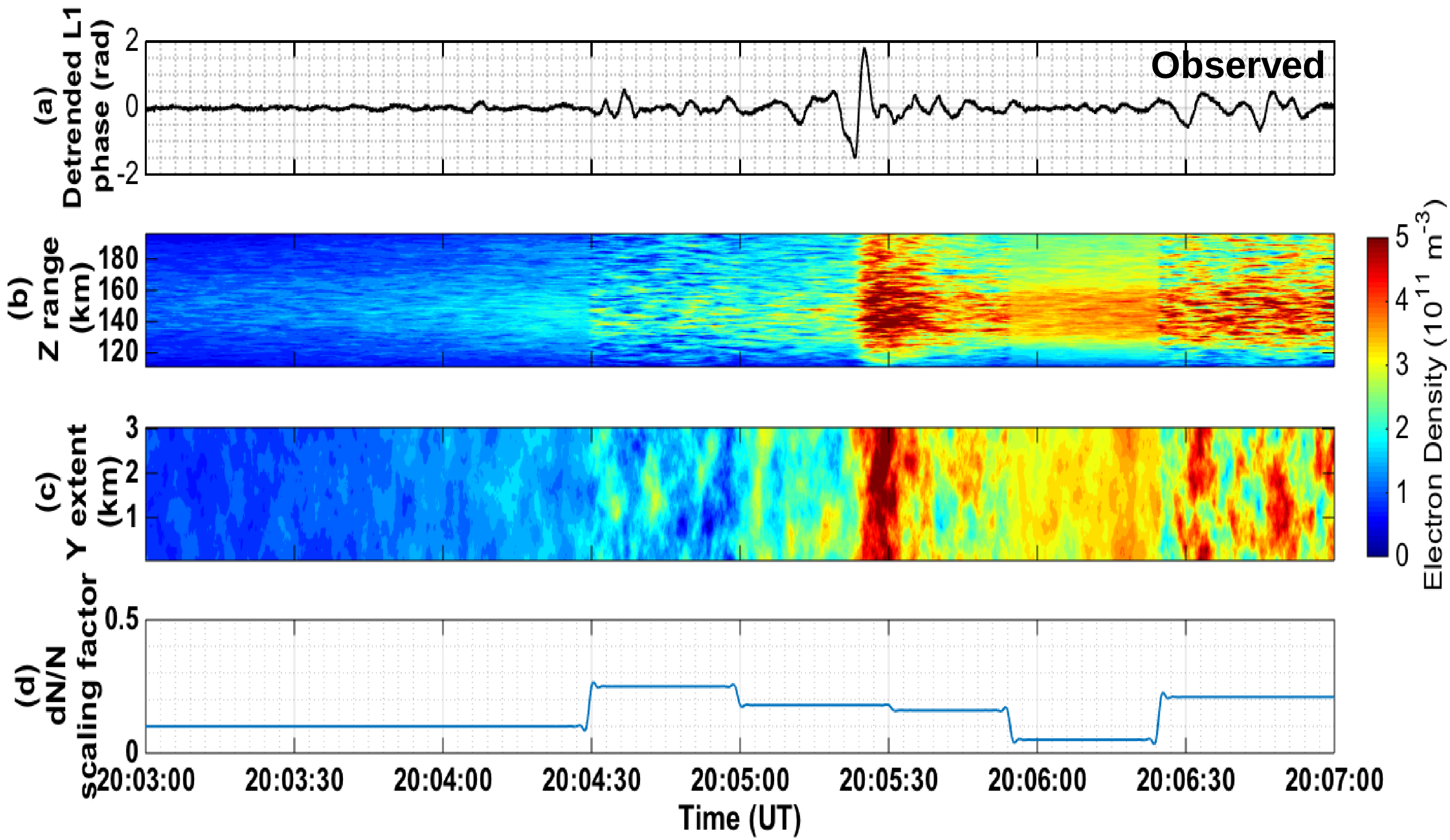

Model-Observation comparison

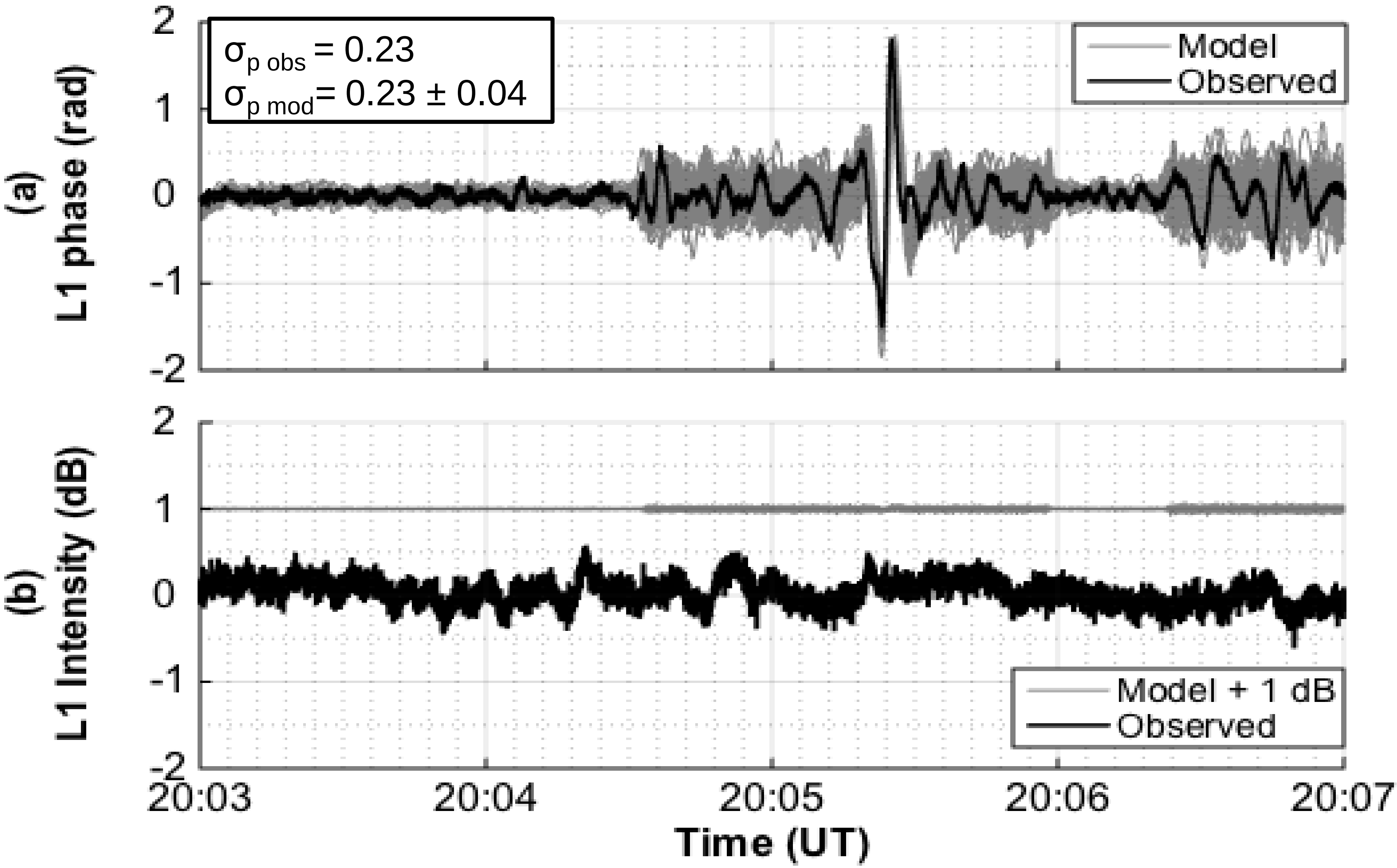

Model-observation comparison

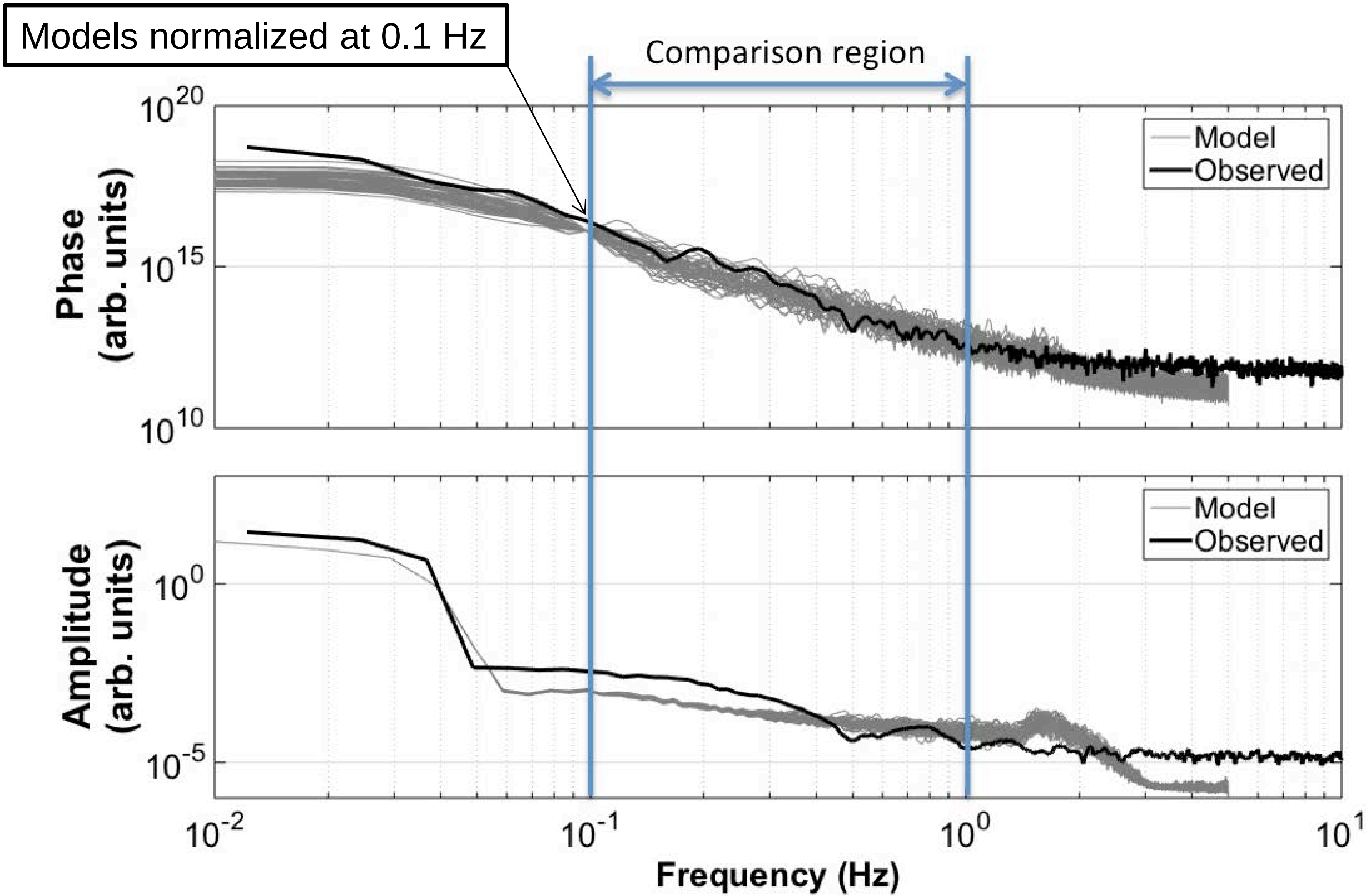

Conclusions

- $\Delta N/N$ is clearly not a constant in this case. Standard deviation varies between 5 - 25 % of mean value specified by EISCAT
- Absence of intensity scintillation observed on line-of-sight approximately 25^{o} off **B**. This is explained as a consequence of high spectral index (4.2) and low axial ratio (1:1)
- The new geometry dramatically reduces computation times to approx. real time and reproduces the observations

References

Chartier, A. T., B. Forte, K. B. Deshpande, G. S. Bust, C. N. Mitchell (**accepted June 2016**), "Three-Dimensional Modeling of High-Latitude Scintillation Observations", Radio Science

Costa, E., & Kelley, M. C. (1977). Ionospheric scintillation calculations based on in situ irregularity spectra. *Radio Science*, *12*(5), 797-809.

Deshpande, K. B., G. S. Bust, C. R. Clauer, C. L. Rino, and C. S. Carrano (2014), Satellite-beacon Ionospheric-scintillation Global Model of the upper Atmosphere (SIGMA) I: High-latitude sensitivity study of the model parameters, J. Geophys. Res. Space Physics, 119, 4026–4043, doi:10.1002/2013JA019699.

Gola, M., A. W. Wernik, S. J. Franke, C. H. Liu, and K. C. Yeh. "Behaviour of HILAT scintillation over Spitsbergen." *Journal of atmospheric and terrestrial physics* 54, no. 9 (1992): 1207-1213.

Knepp, D. L. (1983), Multiple phase-screen calculation of the temporal behavior of stochastic waves, Proc. IEEE, 71(6), 722–737.

Rino, C. L. (1979). A power law phase screen model for ionospheric scintillation: 1. Weak scatter. *Radio Science*, *14*(6), 1135-1145.